The Covalent Trimethoprim Chemical Tag Facilitates Single Molecule Imaging with Organic Fluorophores

Tracy Y. Wang,[†] Larry J. Friedman,[‡] Jeff Gelles,[‡] Wei Min,[†] Aaron A. Hoskins,[§] and Virginia W. Cornish[†]*
[†]Department of Chemistry, Columbia University, New York, New York; [‡]Department of Biochemistry, Brandeis University, Waltham, Massachusetts; and [§]Department of Biochemistry, University of Wisconsin, Madison, Wisconsin

ABSTRACT Chemical tags can be used to selectively label proteins with fluorophores that have high photon outputs. By permitting straightforward single molecule (SM) detection and imaging with organic fluorophores, chemical tags have the potential to advance SM imaging as a routine experimental tool for studying biological mechanism. However, there has been little characterization of the photophysical consequences of using chemical tags with organic fluorophores. Here, we examine the effect the covalent trimethoprim chemical tag (A-TMP-tag) has on the SM imaging performance of the fluorophores, Atto655 and Alexa647, by evaluating the photophysical properties of these fluorophores and their A-TMP-tag conjugates. We measure SM photon flux, survival lifetime, and total photon output under conditions that mimic the live cell environment and demonstrate that the A-TMP-tag complements the advantageous SM imaging properties of Atto655 and Alexa647. We also measure the ensemble properties of quantum yield and photostability lifetime, revealing a correlation between SM and ensemble properties. Taken together, these findings establish a systematic method for evaluating the impact chemical tags have on fluorophores for SM imaging and demonstrate that the A-TMP-tag with Atto655 and Alexa647 are promising reagents for biological imaging.

INTRODUCTION

Single molecule (SM) imaging of biomolecules has transformed our ability to probe biology (1–4). Over the past decade, SM imaging has provided insights into the molecular mechanism of motor protein walking (5), conformational transitions of the ribosome (6), and structural heterogeneity in enzyme catalysis (7), among others (8–12). However, these studies often rely on reconstituted pathways, which are not representative of native cell conditions and not suitable for investigating biological processes such as spliceosome (13), replisome (14), and protein kinase signaling activity (15). Broadly accessible SM imaging in live cells or whole-cell extracts would be transformative for studying biological mechanism, but requires the ability to selectively label proteins with bright and photostable fluorophores that can overcome background and cellular autofluorescence. Fluorescent proteins (FPs) are genetically encoded and inherently selective, but generally lack sufficient photon output for SM imaging. Although the best organic fluorophores have nearly an order of magnitude greater photon output than the FPs (5,16–20), they lack labeling selectivity. By combining genetic encoding with the advantages of organic fluorophores, chemical tags can overcome the need for selective fluorescent labels in SM imaging.

Chemical tags fluorescently label proteins for high performance imaging applications by genetically fusing proteins to a polypeptide that binds to an organic fluorophore. The modularity of the chemical tags allows labeling with a wide variety of commercially available organic fluorophores with similar selectivity as the FPs (21,22). Chemical tags, such as the TMP-tag (23), SNAP-tag (24), and Halo-tag (25) have been used extensively for biological imaging, including live cell SM super resolution imaging (26–28). Based on the high affinity interaction between trimethoprim (TMP) and *Escherichia coli* dihydrofolate reductase (eDHFR) (23), the covalent TMP-tag (A-TMP-tag), is particularly well-suited for SM imaging (Fig. 1 *A*). Target proteins are tagged with eDHFR that has an engineered cysteine nucleophile outside the TMP-binding pocket (eDHFR:L28C) and covalently labeled by an acrylamide-TMP-fluorophore (A-TMP-fluorophore) via a proximity-induced Michael reaction between the cysteine and the acrylamide following TMP-eDHFR binding (29,30). The selectivity and fast labeling kinetics of the A-TMP-tag has permitted high resolution live cell imaging of both nuclear and cytoplasmic proteins (30). Permanent labeling by the A-TMP-tag can expand the use of the noncovalent TMP-tag, which has established SM imaging capabilities in studies of spliceosome assembly in whole-cell yeast extracts (31) and demonstrations of super resolution imaging of nuclear H2B in live cells (27). Combining the advantage of covalent labeling with the performance of the noncovalent TMP-tag, the A-TMP-tag meets the rigorous demands for selectively labeling proteins with organic fluorophores for SM imaging.

Broad application of the A-TMP-tag and other chemical tags for SM imaging is dependent on the tags maintaining the photophysical properties of the organic fluorophores used with them. Although the chemical tags are assumed to not impact the properties of organic fluorophores, the tags introduce alterations to both chemical structure and local environment that can significantly impact a

Submitted August 30, 2013, and accepted for publication November 25, 2013.

*Correspondence: vc114@columbia.edu

Editor: Ashok Deniz.

0006-3495/14/01/0272/7 $2.00

http://dx.doi.org/10.1016/j.bpj.2013.11.4488

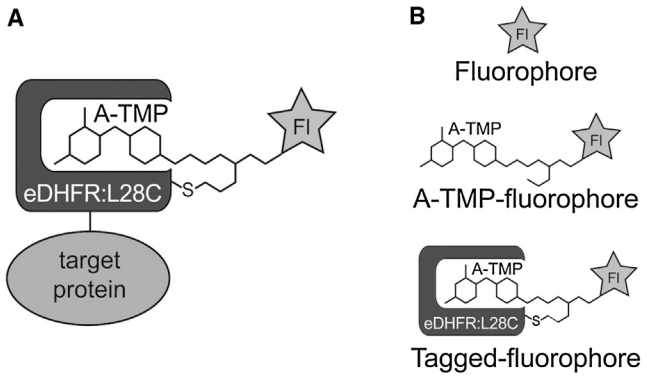

FIGURE 1 (*A*) Schematic cartoon of the covalent trimethoprim chemical tag (A-TMP-tag). A target protein is tagged with an *E. coli* dihydrofolate reductase cysteine mutant (eDHFR:L28C) and covalently bound to a cell-permeable acrylamide-trimethoprim-fluorophore (A-TMP-fluorophore). (*B*) Schematic of fluorophores and their A-TMP-tag conjugates examined in this investigation.

fluorophore's SM imaging capabilities. With the A-TMP-tag, fluorophore conjugation to the electron-rich small molecule A-TMP may cause quenching by intramolecular electron transfer, which has been previously observed with fluorophores conjugated to O^6-benzylguanine in SNAP-tag (32,33). Furthermore the A-TMP-fluorophore is covalently bound to the eDHFR:L28C protein. Although protein binding may recover quenched fluorescence, as in the case of SNAP-tag (32,33), the fluorophore may remain quenched by proximity to electron-rich amino acid residues such as tryptophan, phenylalanine, tyrosine, and/or histidine (34–37). These interactions and other effects caused by the A-TMP-tag, such as sterics, local polarity, and electrostatics, may considerably influence fluorophore photon output and resultant SM imaging performance.

Systematic evaluation of the photophysical properties of fluorophores with chemical tags is crucial to realizing the potential of the tags for SM imaging. To understand the impact chemical and environmental modifications of the A-TMP-tag have on fluorophore SM imaging performance, we measure both SM and ensemble properties of fluorophores, fluorophores conjugated to A-TMP (A-TMP-fluorophore), and fluorophores conjugated to A-TMP bound to eDHFR:L28C (tagged fluorophore) (Fig. 1 *B*). Because overcoming cellular autofluorescence and background noise while minimizing photobleaching are major challenges for biological SM imaging, we focus our investigation on properties corresponding to brightness and photostability. We determine SM photon flux, survival lifetime, and total photon output under different buffer conditions that mimic the intracellular environment. Because SM measurements are technically challenging and require specialized imaging equipment to perform, we sought to measure ensemble properties that could serve as indicators of photon flux and survival lifetime. As a result, we also measure quantum yield and ensemble photostability lifetime. Although ensemble properties are not equivalents for SM properties, correlation between these properties indicates that ensemble measurements can be adapted for more rapid screening of fluorophores and chemical tags that are suitable for SM imaging. We focus our investigation on two fluorophores, an oxazine, Atto655, and a cyanine, Alexa647, because these two fluorophores were used with chemical tags to label nuclear H2B and clathrin-coated pits in the cytosol in demonstrations of live cell SM super resolution imaging (26,27). Studying these fluorophores with the A-TMP-tag gives insights into the properties that allow for successful SM imaging. We assess the impact of the A-TMP-tag on fluorophore SM imaging performance by comparing the SM and ensemble properties of Atto655, Alexa647, and their A-TMP-tag conjugates.

MATERIALS AND METHODS

Chemical synthesis

Chemical structures of fluorophores and A-TMP-fluorophores are shown in Fig. S1 in the Supporting Material. Alexa647-NHS ester (Invitrogen, Grand Island, NY), Atto655-NHS ester (Atto tec, Siegen, Germany), Atto680 NHS ester (Atto tec), and Cy3 NHS ester (GE Life Sciences, Piscataway, NJ) were used without further purification to characterize unmodified fluorophores and synthesize A-TMP-fluorophore conjugates. Atto655-biotin was purchased from Sigma and used without further purification for SM experiments.

A-TMP was synthesized as previously described (30). A-TMP-fluorophores were synthesized by adding 1 mg of fluorophore NHS ester to 500 μL DMF, 1 equivalent of A-TMP, and 5 μL triethylamine (Fig. S1). The mixture was stirred at room temperature for 16 h before being concentrated. A-TMP-fluorophores were purified by reverse phase HPLC. Alexa647-biotin for SM experiments was synthesized by adding 1 mg Alexa647 NHS ester and 1 mg Amine-PEG2-amine (Thermo Scientific, Waltham, MA) with 5 μL triethylamine in DMF. The mixture was stirred at room temperature for 16 h before being concentrated. The reaction was purified by reverse phase HPLC.

Protein expression, purification, labeling, and biotinylation

The vector encoding eDHFR:L28C for *E. coli* overexpression and protein purification has been previously published (29). Plasmids were expressed in BL21(DE3) pLysS cells (Invitrogen). Cells were grown at 37°C to an OD_{600} of 0.6, induced with 0.4 mM IPTG for 3 h, and purified using a nickel sepharose column (HisTrap HP, GE Life Sciences). The protein was dialyzed to phosphate buffered saline (PBS) at 4°C, snap frozen, and stored at −80°C.

For preparation of tagged-fluorophores, 200 μM eDHFR:L28C in PBS was thawed at 4°C and incubated with 1 mM A-TMP-fluorophore and 1 mM NADPH (Sigma Aldrich, Saint Louis, MO) for 2 h (Fig. S1 and Fig. S2). Unlabeled A-TMP-fluorophore was separated from tagged-fluorophores using 7000 MWCO Zeba desalting spin column (Thermo Scientific) equilibrated with PBS.

The vector encoding of eDHFR:L28C-bioseq, for *E. coli* expression and protein purification has been previously published (38). eDHFR:L28C expression and purification were carried our as previously described (39). eDHFR:L28C-bioseq biotinylation was carried out as previously described (39,40). Biotinylated eDHFR:L28C was dialyzed to PBS at 4°C, snap frozen and stored at −80°C, and thawed at 4°C before use in SM experiments. For preparation of biotinylated tagged-fluorophores, 1 μM

biotinylated eDHFR:L28C with 2 μM A-TMP-Atto655 or A-TMP-Alexa647, and 2 μM NADPH in PBS was incubated for 2 h and used for imaging without further separation.

Single molecule methods

Single molecule imaging of fluorophore-biotin and biotinylated tagged-fluorophores was performed on a homebuilt total internal reflection fluorescence (TIRF) microscope. Samples were immobilized on glass slides passivated with PEG and PEG-streptavidin. Samples were excited with a 633 nm laser at 250 μWatt and imaged until at least 90% of molecules were photobleached. Photostability survival time was calculated by plotting the individual traces of 300–500 individual molecules, identifying the photobleaching times, and fitting those times to a maximum likelihood single exponential fit of survival times. Photon flux was measured by picking 10–20 well-resolved single molecules and integrating the total Gaussian fluorophore signal over time. The background, as determined by the average signal after photobleaching, was subtracted from the average fluorescence signal. The resulting signal was converted to photon flux using the ADU conversion factor that had been determined for that camera using the calibration protocol previously described (41). Total photon output was calculated by multiplying photon flux by survival lifetime.

Ensemble methods

The quantum yields were determined using the comparative method (42). Aqueous solutions of fluorophore, A-TMP-fluorophore, and tagged-fluorophore in PBS buffer were diluted to absorbances <0.1 to prevent inner filter effects. Absorbance measurements and spectra were measured using a Tecan Infinite 200 and fluorescence measurements and spectra were obtained with a Horiba Scientific Fluorolog-3 spectrofluorometer. The slope of the plot of fluorescence emission compared to absorbance was compared to that of a quantum yield reference solution under the same excitation and collection conditions. This measurement was repeated in triplicate for each fluorophore. Fluorescence quantum yield standards used were cresyl violet in methanol and Nile blue in methanol.

Photobleaching time constants were determined using a microdroplet photobleaching assay, similar to one used by Tsien and co-workers (43). Aqueous microdroplets of fluorophore, A-TMP-fluorophore, and tagged-fluorophore in PBS buffer were created under mineral oil that had been previously extracted with PBS buffer. The microdroplets were bleached using laser excitation (532 or 633 nm) such that the laser beam incidence was greater than the size of individual droplets.

The absorbance and emission spectra for fluorophores and their A-TMP-tag conjugates were measured and recorded in Table S3. We observed no differences between fluorophores and their A-TMP-tag conjugated for all fluorophores.

RESULTS AND DISCUSSION

SM total photon output

To examine the effect the A-TMP-tag has on SM imaging performance, we determine the total photon output of fluorophores and tagged-fluorophores (Fig. 1 *B*). Using TIRF microscopy, we measure SM photon flux and survival lifetime, which are used to calculate total photon output. The need to biotinylate fluorophores for biotin-streptavidin immobilization in TIRF microscopy limits our SM evaluation to fluorophores and tagged-fluorophorea. Photon flux and survival lifetimes for fluorophores and tagged-fluorophores are measured in PBS buffer, PBS buffer containing 10 mM β-mercaptoethylamine (MEA) to reproduce the reducing environment of the cell, and PBS containing 40% whole-cell yeast extract (YE) to reproduce the macromolecular density of the cell. SM photon fluxes and survival lifetimes for fluorophores and tagged-fluorophores for Atto655 and Alexa647 are displayed in Fig. 2 and Table S1.

Differences in photon flux and survival lifetimes between fluorophores and tagged-fluorophores are generally within 50% and vary between buffer conditions. The photon fluxes of the tagged-fluorophores are either the same or lower than those of their counterparts. In PBS, the tagged-fluorophores have no differences in photon flux from the fluorophores. On the other hand, in YE, the tagged-fluorophores have 30% lower photon fluxes than those of the fluorophores. In MEA, tagged-Atto655 has the same photon flux as that of Atto655 but tagged-Alexa647 has a 20% lower photon flux than that of Alexa647.

The survival lifetimes of the tagged-fluorophores are either higher or lower than those of the fluorophores. In PBS, tagged-Atto655 has a 30% shorter survival lifetime than that of Atto655, whereas tagged-Alexa647 has a 20% longer survival lifetime than that of Alexa647. In the presence of MEA, the tagged-fluorophores have longer survival lifetimes than those of the fluorophores, with 50% longer survival lifetime for tagged-Atto655 and a 30% longer survival lifetime for tagged-Alexa647. In YE, the

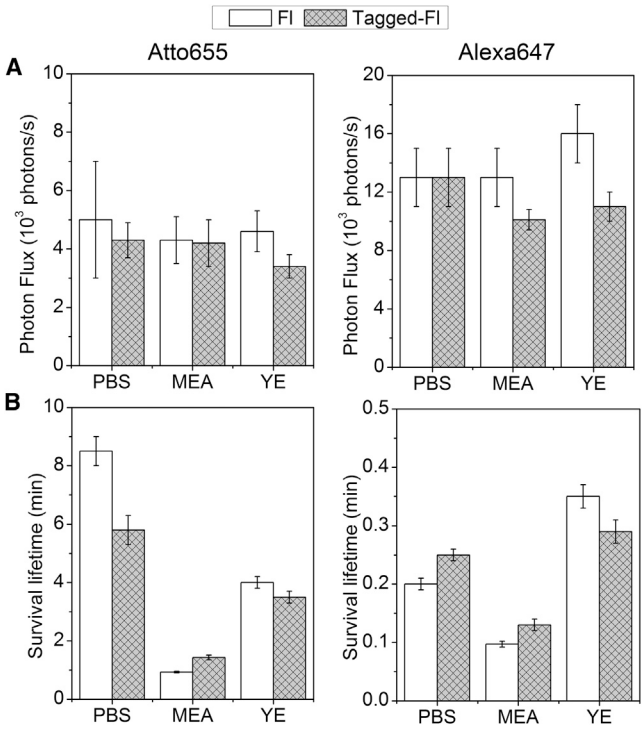

FIGURE 2 SM photon fluxes and survival lifetimes of fluorophores (Fl) and tagged-fluorophores (Tagged-Fl) for Atto655 and Alexa647 in PBS buffer, 10 mM MEA, and 40% YE with 250 μW 633 nm laser illumination. (*A*) SM photon flux, which is determined by the number of detected photons. (*B*) Average SM survival lifetime before photobleaching.

tagged-fluorophores have 20% and 10% shorter survival lifetimes than those of the fluorophores for Atto655 and Alexa647, respectively.

The fluorophores have greater differences in photon flux and survival lifetime between buffer conditions than between fluorophore and tagged-fluorophores in the same conditions. Both Atto655 and Alexa647 have lower survival lifetimes in MEA than those in PBS, with the survival lifetime of Atto655 in MEA nearly an order of magnitude less than that in PBS. Although the survival lifetime of Atto655 in YE is less than half of that in PBS, the survival lifetime of Alexa647 in YE is 30% longer than that in PBS. The fluorophores have no differences in photon flux between the buffer conditions. Overall, the photon fluxes of Alexa647 are two to three times higher than those of Atto655 across the investigated conditions. However, the survival lifetimes of Atto655 are nearly an order of magnitude greater than those of Alexa647.

SM total photon flux for fluorophores and tagged-fluorophores for Atto655 and Alexa647 are displayed in Fig. 3 and Table S2. Although the tagged fluorophores exhibit some differences in photon flux and survival lifetime from the fluorophores, the total photon outputs of the tagged-fluorophores is the same or on the same order of magnitude as those of the fluorophores. The total photon outputs of tagged-Atto655 are the same as Atto655 across all the investigated conditions. The total photon outputs of tagged-Alexa647 are the same as Alexa647 in PBS and in MEA. Alexa647 in YE is the only fluorophore that exhibits a difference in photon output between the fluorophore and the tagged-fluorophore, with the tagged-Alexa647 having 30% less photon output than that of Alexa647. However, the photon output of tagged-Alexa647 in YE is the same as the photon output of both Alexa647 and tagged-Alexa647 in PBS. The TMP-tag does not affect the overall SM imaging performance of Atto655 and Alexa647.

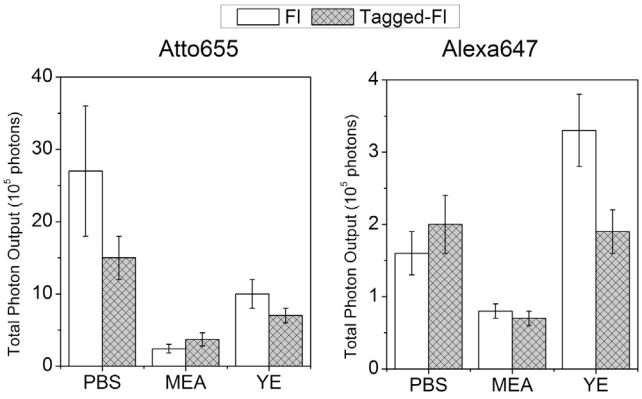

FIGURE 3 Total photon output of fluorophores (Fl) and tagged-fluorophores (Tagged-Fl) for Atto655 and Alexa647 in PBS buffer, 10 mM MEA, and 40% YE with 250 μW 633 nm laser illumination. Total photon output is determined by multiplying photon flux by average survival lifetime.

Overall, the total photon output of Atto655 is approximately an order of magnitude greater than that of Alexa647. Atto655 has the greatest photon output in PBS, which is 2,700,000 $\pm$ 900,000 photons. However, in YE, Atto655 photon output is 60% less than the output in PBS. Alexa647 has the greatest photon output in YE at 330,000 $\pm$ 50,000 photons, which is nearly double the photon output in PBS. Both fluorophores have the lowest photon output in MEA, with Atto655 having nearly an order of magnitude lower output than that in PBS and Alexa647 having nearly half the output than that in PBS.

Quantum yield and ensemble photostability lifetime

We measure the quantum yields and photostability lifetimes of Atto655, Alexa647, and their corresponding A-TMP-fluorophores and tagged-fluorophores (Fig. 1 *B*) to examine the correlation between ensemble and SM properties. We also perform ensemble measurements on an additional oxazine, Atto680, and cyanine, Cy3, to more broadly understand the impacts of the A-TMP-tag on oxazines and cyanines. The ensemble properties of these fluorophores and their A-TMP-tag conjugates in PBS buffer are shown in Fig. 4 and Table S3.

The two fluorophore classes exhibit trends in quantum yield and photostability lifetime between the fluorophores and their A-TMP-tag conjugates. For Atto655 and Atto680, the tagged-oxazines have the same quantum yields as the oxazines even though the A-TMP-oxazines have lower quantum yields. However, the photostability lifetimes of the A-TMP-oxazines and tagged-oxazines are both shorter than those of the oxazines. For Alexa647 and Cy3, the A-TMP-cyanines and the tagged-cyanines have greater or the same quantum yields as the cyanines. Although the tagged-cyanines have shorter photostability lifetimes than those of the A-TMP-cyanines, they are still longer than those of the cyanines.

Overall, the tagged-fluorophores have the same if not better quantum yield than the fluorophores. Although the tagged-cyanines are more photostable than the cyanines, the tagged-oxazines are less photostable than the oxazines. The A-TMP-tag does not affect the ensemble photophysical properties of the cyanines or the quantum yield of oxazines, but does reduce the photostability of the oxazines. Alexa647 has the highest quantum yield, but is the least photostable out of the examined fluorophores. Atto680, Atto655, and Cy3 are approximately an order of magnitude more photostable than Alexa647, with Atto680 being the most photostable.

DISCUSSION

These results establish that the A-TMP-tag complements the advantageous SM imaging properties of Atto655 and Alexa647, facilitating SM imaging with these fluorophores. Based on the SM examination of these fluorophores and

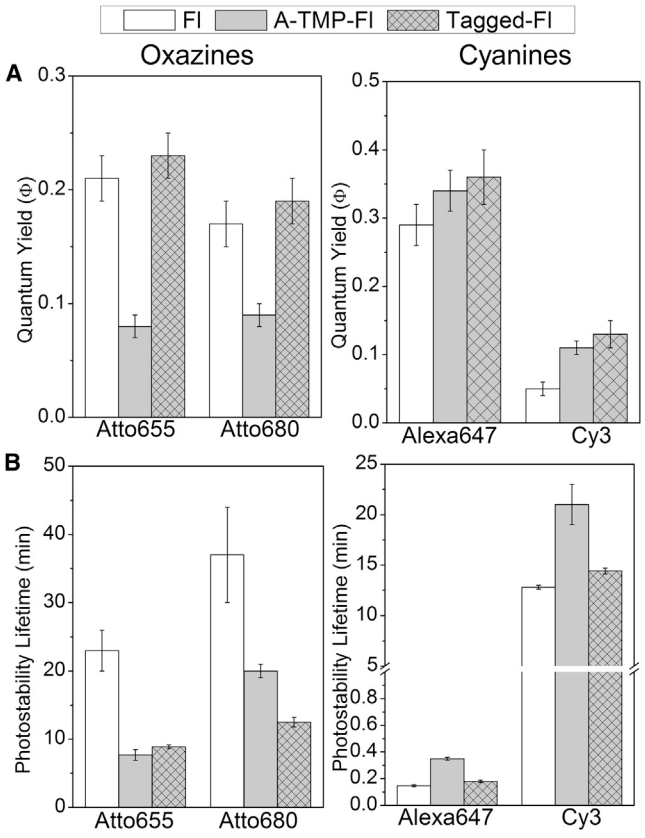

FIGURE 4 Quantum yield and photostability lifetime for fluorophores (Fl), A-TMP-fluorophore (A-TMP-Fl) and tagged-fluorophores (Tagged-Fl) for Atto655 and Alexa647 in PBS buffer. (*A*) Quantum yield. (*B*) Photostability lifetime is the half-life of fluorescence signal due to photobleaching.

their tagged-counterparts under buffers that mimic the reducing potential and macromolecular density of the cell, we determine that the A-TMP-tag has buffer-dependent effects on photon flux and survival lifetime. However, the A-TMP-tag does not affect total photon output in most cases. Although the A-TMP-tag lowers Alexa647 photon output in YE, this output is the same as that for Alexa647 in PBS. With the best organic fluorophores having photon outputs ~10-fold greater than the best FPs (5,16–20), the A-TMP-tag's preservation of Atto655 and Alexa647 photon output is significant for upholding these fluorophores' SM imaging performances. These findings also reveal that Atto655 is superior to Alexa647 for imaging on longer timescales, with survival lifetimes and total photon outputs nearly an order of magnitude greater than those of Alexa647. At the same time, the photon fluxes of Alexa647 are two to three times greater than those of Atto655, making Alexa647 better suited for applications requiring positional localization (44). The comparative advantages of survival lifetime and photon flux between these two fluorophores are not altered by the A-TMP-tag, further indicating that the A-TMP-tag is a valuable tool for labeling proteins for SM imaging applications.

These findings reflect Atto655 and Alexa647 performance for SM imaging and highlight the importance of fluorophore characterization under different conditions. Recent studies of fluorophore performance in various buffer conditions (45) and in fixed cells (46) have begun to provide guidelines for selecting appropriate fluorophores for SM and super resolution imaging. Our investigation goes a step further by characterizing fluorophores with chemical tags under conditions that imitate those of the live cell. Although we examine fluorophores in a reducing environment and a macromolecularly dense environment, we do not include oxygen scavengers because these conditions are not representative of the native, live cell. As a result, the measured photon output of Alexa647 in this study is lower than that of Atto655, which is the opposite of what has been previously observed with these fluorophores in low oxygen, super resolution SM imaging conditions (46). Although differences in photon output can vary between experimental setups, Alexa647's lower photon output in this investigation is likely attributed to its sensitivity to photooxidative bleaching as a cyanine (47,48) along with the use of nondeoxygenated buffers. These results suggest that Atto655 may be more advantageous for oxygenated conditions in live cell imaging, but further investigation is needed to account for fluorophore interactions in cell environments, such as nonspecific binding, which may further impact imaging performance.

Ensemble evaluation of fluorophores gives valuable insights regarding the use of ensemble properties as indicators of SM imaging performance. As a measure of the probability of fluorescence emission, quantum yield is not an ensemble equivalent of photon flux, which is the rate of photon emission from the fluorophore. Although photostability lifetime and survival lifetime are both direct measures of photostability, differences in illumination intensities and imaging conditions can affect these lifetimes as high illumination causes fluorophores to experience more dark state transitions from which they are photobleached (43,49,50). However, we do observe a correlation between the ensemble and SM properties as both Atto655 and Alexa647 experience no changes in quantum yield and photon flux with the addition of the A-TMP-tag in PBS. In addition, the A-TMP-tag lowers both photostability lifetime and survival lifetime for Atto655, whereas the tag raises Alexa647 photostability lifetime and survival lifetime. The ability to measure ensemble properties without specialized equipment and the correlation between the ensemble and SM properties indicates that these ensemble measurements can be applied for wider screenings of chemically tagged fluorophores with advantageous properties that can be later confirmed by SM investigation.

Ensemble measurements also allow separate examination of chemical and environmental effects from the A-TMP-tag because the properties of fluorophores, A-TMP-fluorophores, and the tagged-fluorophores can be measured individually. With the oxazines Atto655 and Atto680, we

observe that the A-TMP-oxazines have lower quantum yields, which is consistent with previous observations of quenching by intramolecular electron transfer after conjugation to an electron-rich molecule in these fluorophores and other oxazines (32,34,51). We also observe that tagged-Atto655 and tagged-Atto680 have quantum yields that are unchanged for the original fluorophores, an effect that was similarly observed with oxazines and the SNAP-tag (32,33), and may be caused by inhibited electron transfer due to the interaction of A-TMP with the eDHFR binding pocket. For the cyanine Cy3, we observe stepwise increases in quantum yield from Cy3, to A-TMP-Cy3, and to tagged-Cy3, which is consistent with the tag causing steric inhibition of *cis-trans* photoisomerization in the methionine chain, a mechanism of nonradiative decay (52,53). Although a similar trend in quantum yield is not observed with the cyanine Alexa647, its longer methionine chain has a lower rate of *cis-trans* isomerization (54,55) that likely reduces the steric effects of the A-TMP-tag on quantum yield. Examining fluorophores with chemical tags using ensemble measurements can provide insights into their interactions and predict whether fluorophores in the same chemical class will behave similarly.

CONCLUSION

Chemical tags are emerging as a strategic experimental tool for selectively labeling proteins with organic fluorophores to meet the demand for fluorescent labels with high photon outputs in SM imaging. As the chemical tags make SM imaging more accessible, there is a growing need for characterization to not only understand the effects the chemical tags have on fluorophores, but also identify chemically tagged fluorophores with suitable properties for SM imaging. We examined both SM and ensemble photophysical properties of the fluorophores, Atto655 and Alexa647, and their A-TMP-tag conjugates. We demonstrated that the A-TMP-tag is an effective labeling reagent for SM imaging because it upholds Atto655 and Alexa647 total photon output. Characterizing these commercially available fluorophores with the A-TMP-tag provides photophysical benchmarks to compare and guide the selection of fluorophores and chemical tags. As the capabilities of chemical tags evolve with the developments of new organic fluorophores and fluorescent materials for biological imaging, this framework can continue to evaluate and identify the most promising fluorophores and chemical tags for SM imaging. By using SM imaging to decipher the complex dynamics of protein function and interaction in live cells, the chemical tags have the potential to revolutionize the study of mechanistic biology.

SUPPORTING MATERIAL

Two figures and three tables are available at http://www.biophysj.org/biophysj/supplemental/S0006-3495(13)05747-0.

We thank Dr. Keewook Paeng for experimental assistance. We also thank Dr. Casey Brown, Dr. Chaoran Jing, and Zhixing Chen for helpful discussions.

The authors declare the following competing financial interest(s): V.W.C. holds patents on the TMP-tag technology, and the technology is licensed and commercialized by Active Motif.

REFERENCES

1. Moerner, W. E. 2007. New directions in single-molecule imaging and analysis. *Proc. Natl. Acad. Sci. USA.* 104:12596–12602.
2. Joo, C., H. Balci, …, T. Ha. 2008. Advances in single-molecule fluorescence methods for molecular biology. *Annu. Rev. Biochem.* 77:51–76.
3. Weiss, S. 1999. Fluorescence spectroscopy of single biomolecules. *Science.* 283:1676–1683.
4. Zhuang, X., L. E. Bartley, …, S. Chu. 2000. A single-molecule study of RNA catalysis and folding. *Science.* 288:2048–2051.
5. Yildiz, A., J. N. Forkey, …, P. R. Selvin. 2003. Myosin V walks hand-over-hand: single fluorophore imaging with 1.5-nm localization. *Science.* 300:2061–2065.
6. Fei, J., J. E. Bronson, …, R. L. Gonzalez, Jr. 2009. Allosteric collaboration between elongation factor G and the ribosomal L1 stalk directs tRNA movements during translation. *Proc. Natl. Acad. Sci. USA.* 106:15702–15707.
7. Lu, H. P., L. Xun, and X. S. Xie. 1998. Single-molecule enzymatic dynamics. *Science.* 282:1877–1882.
8. Yu, J., J. Xiao, …, X. S. Xie. 2006. Probing gene expression in live cells, one protein molecule at a time. *Science.* 311:1600–1603.
9. Schuler, B., E. A. Lipman, and W. A. Eaton. 2002. Probing the free-energy surface for protein folding with single-molecule fluorescence spectroscopy. *Nature.* 419:743–747.
10. Myong, S., I. Rasnik, …, T. Ha. 2005. Repetitive shuttling of a motor protein on DNA. *Nature.* 437:1321–1325.
11. Elf, J., G.-W. Li, and X. S. Xie. 2007. Probing transcription factor dynamics at the single-molecule level in a living cell. *Science.* 316:1191–1194.
12. Funatsu, T., Y. Harada, …, T. Yanagida. 1995. Imaging of single fluorescent molecules and individual ATP turnovers by single myosin molecules in aqueous solution. *Nature.* 374:555–559.
13. Crawford, D. J., A. A. Hoskins, …, M. J. Moore. 2008. Visualizing the splicing of single pre-mRNA molecules in whole cell extract. *RNA.* 14:170–179.
14. Shen, Z., A. Chakraborty, …, S. G. Prasanth. 2012. Dynamic association of ORCA with prereplicative complex components regulates DNA replication initiation. *Mol. Cell. Biol.* 32:3107–3120.
15. Jain, A., R. Liu, …, T. Ha. 2011. Probing cellular protein complexes using single-molecule pull-down. *Nature.* 473:484–488.
16. Fernández-Suárez, M., and A. Y. Ting. 2008. Fluorescent probes for super-resolution imaging in living cells. *Nat. Rev. Mol. Cell Biol.* 9:929–943.
17. Xia, T., N. Li, and X. Fang. 2013. Single-molecule fluorescence imaging in living cells. *Annu. Rev. Phys. Chem.* 64:459–480.
18. Yildiz, A., and P. R. Selvin. 2005. Fluorescence imaging with one nanometer accuracy: application to molecular motors. *Acc. Chem. Res.* 38:574–582.
19. Schmidt, T., U. Kubitscheck, …, U. Nienhaus. 2002. Photostability data for fluorescent dyes: an update. *Single Molecules.* 3:327.
20. Sako, Y., S. Minoghchi, and T. Yanagida. 2000. Single-molecule imaging of EGFR signalling on the surface of living cells. *Nat. Cell Biol.* 2:168–172.
21. Wombacher, R., and V. W. Cornish. 2011. Chemical tags: applications in live cell fluorescence imaging. *J. Biophotonics.* 4:391–402.

22. Jing, C., and V. W. Cornish. 2011. Chemical tags for labeling proteins inside living cells. *Acc. Chem. Res.* 44:784–792.

23. Miller, L. W., Y. Cai, …, V. W. Cornish. 2005. In vivo protein labeling with trimethoprim conjugates: a flexible chemical tag. *Nat. Methods.* 2:255–257.

24. Keppler, A., S. Gendreizig, …, K. Johnsson. 2003. A general method for the covalent labeling of fusion proteins with small molecules in vivo. *Nat. Biotechnol.* 21:86–89.

25. Los, G. V., L. P. Encell, …, K. V. Wood. 2008. HaloTag: a novel protein labeling technology for cell imaging and protein analysis. *ACS Chem. Biol.* 3:373–382.

26. Jones, S. A., S.-H. Shim, …, X. Zhuang. 2011. Fast, three-dimensional super-resolution imaging of live cells. *Nat. Methods.* 8:499–508.

27. Wombacher, R., M. Heidbreder, …, M. Sauer. 2010. Live-cell super-resolution imaging with trimethoprim conjugates. *Nat. Methods.* 7:717–719.

28. Wilmes, S., M. Staufenbiel, …, J. Piehler. 2012. Triple-color super-resolution imaging of live cells: resolving submicroscopic receptor organization in the plasma membrane. *Angew. Chem. Int. Ed. Engl.* 51:4868–4871.

29. Gallagher, S. S., J. E. Sable, …, V. W. Cornish. 2009. An in vivo covalent TMP-tag based on proximity-induced reactivity. *ACS Chem. Biol.* 4:547–556.

30. Chen, Z., C. Jing, …, V. W. Cornish. 2012. Second-generation covalent TMP-tag for live cell imaging. *J. Am. Chem. Soc.* 134:13692–13699.

31. Hoskins, A. A., L. J. Friedman, …, M. J. Moore. 2011. Ordered and dynamic assembly of single spliceosomes. *Science.* 331:1289–1295.

32. Stöhr, K., D. Siegberg, …, D.-P. Herten. 2010. Quenched substrates for live-cell labeling of SNAP-tagged fusion proteins with improved fluorescent background. *Anal. Chem.* 82:8186–8193.

33. Sun, X., A. Zhang, …, I. R. Corrêa, Jr. 2011. Development of SNAP-tag fluorogenic probes for wash-free fluorescence imaging. *ChemBioChem.* 12:2217–2226.

34. Marmé, N., J.-P. Knemeyer, …, J. Wolfrum. 2003. Inter- and intramolecular fluorescence quenching of organic dyes by tryptophan. *Bioconjug. Chem.* 14:1133–1139.

35. Chen, H., S. S. Ahsan, …, W. W. Webb. 2010. Mechanisms of quenching of Alexa fluorophores by natural amino acids. *J. Am. Chem. Soc.* 132:7244–7245.

36. Abe, R., H. Ohashi, …, H. Ueda. 2011. "Quenchbodies": quench-based antibody probes that show antigen-dependent fluorescence. *J. Am. Chem. Soc.* 133:17386–17394.

37. Buschmann, V., K. D. Weston, and M. Sauer. 2003. Spectroscopic study and evaluation of red-absorbing fluorescent dyes. *Bioconjug. Chem.* 14:195–204.

38. Zhang, Z., P. T. R. Rajagopalan, …, G. G. Hammes. 2004. Single-molecule and transient kinetics investigation of the interaction of dihydrofolate reductase with NADPH and dihydrofolate. *Proc. Natl. Acad. Sci. USA.* 101:2764–2769.

39. Antikainen, N. M., R. D. Smiley, …, G. G. Hammes. 2005. Conformation coupled enzyme catalysis: single-molecule and transient kinetics investigation of dihydrofolate reductase. *Biochemistry.* 44:16835–16843.

40. Miller, G. P., and S. J. Benkovic. 1998. Deletion of a highly motional residue affects formation of the Michaelis complex for *Escherichia coli* dihydrofolate reductase. *Biochemistry.* 37:6327–6335.

41. Friedman, L. J., J. Chung, and J. Gelles. 2006. Viewing dynamic assembly of molecular complexes by multi-wavelength single-molecule fluorescence. *Biophys. J.* 91:1023–1031.

42. Williams, A. T. R., S. A. Winfield, and J. N. Miller. 1983. Relative fluorescence quantum yields using a computer-controlled luminescence spectrometer. *Analyst (Lond.).* 108:1067–1071.

43. Tsien, R. Y., L. Ernst, and A. Waggoner. 2006. Fluorophores for confocal microscopy: photophysics and photochemistry. *In* Handbook of Biological Confocal Microscopy. J. B. Pawley, editor. New York, Springer, pp. 338–352.

44. Huang, B., M. Bates, and X. Zhuang. 2009. Super-resolution fluorescence microscopy. *Annu. Rev. Biochem.* 78:993–1016.

45. Kasper, R., M. Heilemann, …, M. Sauer. 2007. *In* Towards Ultra-Stable Fluorescent Dyes for Single-Molecule Spectroscopy, J. Popp and G. von Bally, editors. Optical Society of America, Washington, DC, pp. 6633–6671.

46. Dempsey, G. T., J. C. Vaughan, …, X. Zhuang. 2011. Evaluation of fluorophores for optimal performance in localization-based super-resolution imaging. *Nat. Methods.* 8:1027–1036.

47. Dave, R., D. S. Terry, …, S. C. Blanchard. 2009. Mitigating unwanted photophysical processes for improved single-molecule fluorescence imaging. *Biophys. J.* 96:2371–2381.

48. Aitken, C. E., R. A. Marshall, and J. D. Puglisi. 2008. An oxygen scavenging system for improvement of dye stability in single-molecule fluorescence experiments. *Biophys. J.* 94:1826–1835.

49. Donnert, G., C. Eggeling, and S. W. Hell. 2007. Major signal increase in fluorescence microscopy through dark-state relaxation. *Nat. Methods.* 4:81–86.

50. Humpolíčková, J., A. Benda, …, M. Hof. 2010. Dynamic saturation optical microscopy: employing dark-state formation kinetics for resolution enhancement. *Phys. Chem. Chem. Phys.* 12:12457–12465.

51. Zhu, R., X. Li, …, A. Yu. 2011. Photophysical properties of Atto655 dye in the presence of guanosine and tryptophan in aqueous solution. *J. Phys. Chem. B.* 115:5001–5007.

52. Aramendia, P. F., R. M. Negri, and E. S. Roman. 1994. Temperature dependence of fluorescence and photoisomerization in symmetric carbocyanines. Influence of medium viscosity and molecular structure. *J. Phys. Chem.* 98:3165–3173.

53. Mishra, A., R. K. Behera, …, G. B. Behera. 2000. Cyanines during the 1990s: a review. *Chem. Rev.* 100:1973–2012.

54. Widengren, J., and P. Schwille. 2000. Characterization of photoinduced isomerization and back-isomerization of the cyanine dye Cy5 by fluorescence correlation Spectroscopy. *J. Phys. Chem. A.* 104:6416–6428.

55. Chibisov, A. K., G. V. Zakharova, and H. Gorner. 1996. Effects of substituents in the polymethine chain on the photoprocesses in indodicarbocyanine dyes. *J. Chem. Soc., Faraday Trans.* 92:4917–4925.